SIMULATIONS OF A POPULATION OF PLANETARY NEBULAE

G. STASINSKA
DAEC, Observatoire de Paris-Meudon, France
and
R. TYLENDA
DAEC, Observatoire de Paris-Meudon, France
Copernicus Astronomical Center, Torun, Poland

ABSTRACT. We present a simulation of the population of Galactic bulge planetary nebulae (GBPN), which matches the diagrams obtained from VLA radio observations. This simulation may not be the only one fitting the observed data, but it helps understanding the role of observational uncertainties and selection effects in the interpretation of observational diagrams.

1. INTRODUCTION

Statistical properties of planetary nebulae (PN) are derived from diagrams in which selection effects and observational uncertainties enter in a complicated manner. In order to understand how they operate, we have performed a numerical experiment, in which we have simulated a population of PN, assumed to be lying in the Galactic bulge. We have then simulated the observing conditions. This enabled us to construct diagrams which are directly comparable to observational ones. The results of such an experiment is presented below.

2. PROCEDURE FOR SIMULATING THE GBPN POPULATION

2.1. The model for a single PN

The schematic model adopted consists in a constant density shell expanding uniformly around a post AGB star which evolves according to the tracks of Schönberner (1979, 1983) and Blöcker and Schönberner (1991). At any time, the ionized mass is computed analytically by balancing the number of ionizing photons and the number of hydrogen recombinations to excited levels.

2.2. Simulation of the GBPN population

Individual model PN are randomly selected out of a uniform distribution for the ages, and a Gaussian distribution for the central star masses as well as for the logarithms of nebular masses and expansion velocities The distance to each nebula is randomly selected from a Gaussian distribution, centered at 7.8Kpc with a standard deviation of 0.8Kpc, appropriate for GBPN.

2.3. Simulation of the observing conditions

In order to understand diagrams obtained from 6cm radio measurements, we must simulate the observing conditions. We assume that logarithmic errors in the fluxes are Gaussian, with a dis-

R. Weinberger and A. Acker (eds.), Planetary Nebulae, 461–464.

persion of 0.05dex , and that the dispersion of errors in the diameters ϕ ranges from 0.15 dex for ϕ=1" to 0.05 dex for ϕ > 10". Since, in order to exclude most of foreground PN, the observed sample of GBPN is defined by eliminating objects having ϕ > 20", the same is done for simulations. Finally, observed and simulated populations must be compared using complete subsamples. This requires taking only PN with F(6cm) > 10mJy (81 objects in the observed sample).

3. AN EXAMPLE OF A MODEL GBPN POPULATION MATCHING THE VLA DATA

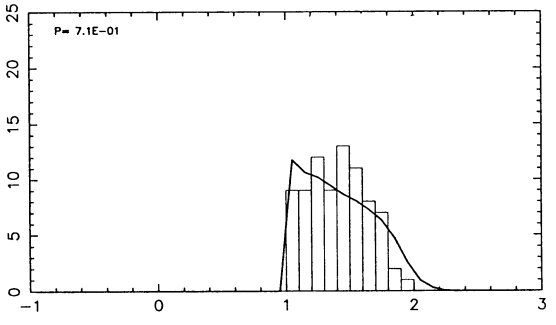

Fig. 1 log F_{6cm} (mJy)

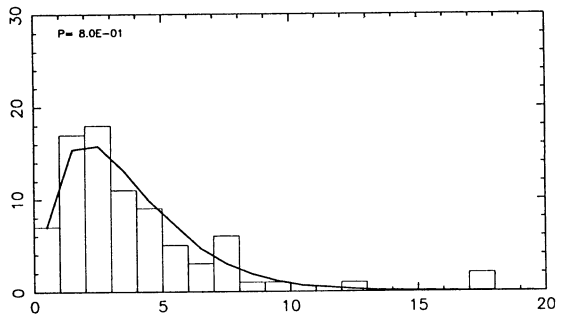

Fig. 2 ϕ (arc sec)

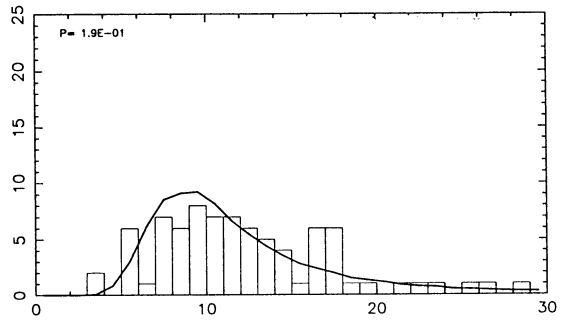

Fig. 3 SHKLOVSKY DISTANCE

We present a few figures relative to a specific model population leading to diagrams that are in agreement with the VLA observations of GBPN published in Zijlstra et al. (1989). In this theoretical population, the central star masses are distributed around 0.57 $M_\odot$ with a standard deviation of 0.02 $M_\odot$; the dispersion of the nebular masses is 0.3 dex around 0.1 $M_\odot$, and that of the expansion velocities v_{exp} is 0.3 dex around 20 km/s.

Figs. 1, 2 and 3 show respectively the distributions of the 6cm fluxes, of the angular diameters, and of the Shklovsky distances (computed assuming an ionized mass of 0.2$M_\odot$). Boxes are histograms relative to observations . Curves represent the simulated distributions. The agreement is good (confirmed by thesignificance of the Kolmogorov-Smirnov test, respectively found to be 0.71, 0.80 and 0.19).

Fig. 4a shows the classical nebular mass-radius diagram for the observed sample, where M_ϕ is calculated using the formula $M_\phi = 3.12\ 10^{-3}\ F(6cm)^{0.5}\phi^{1.5}$. The observed points gather along a line of slope 1.5. This is often interpreted as the consequence of the gradual ionization of the expanding nebulae. In

https://doi.org/10.1017/S0074180900172067 Published online by Cambridge University Press

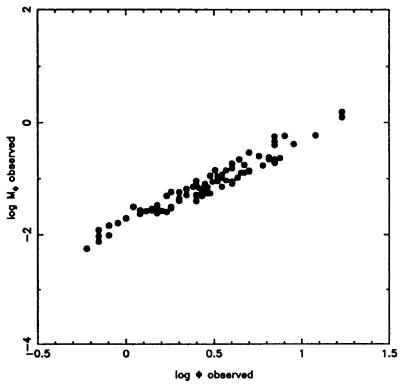

Fig. 4a

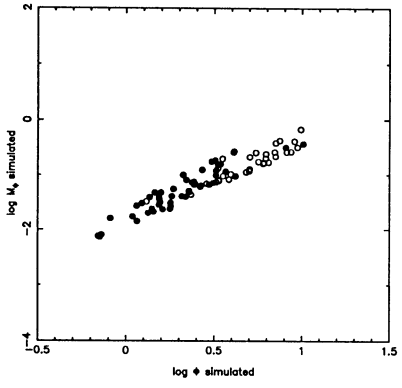

Fig. 4b

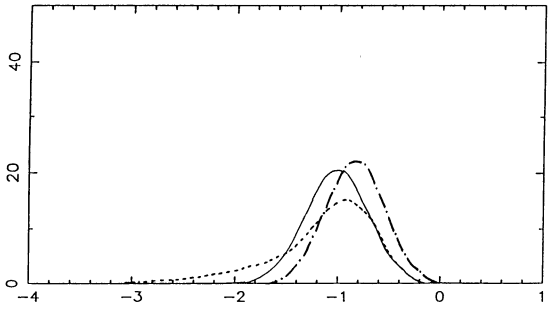

Fig. 5 log M_{neb}

fact, it has already been shown by Stasińska et al (1989) that the aspect of this diagram is mainly the result of the formal dependance of M_ϕ on ϕ. Fig. 4b shows the same diagram for the simulated population. White circles represent density bounded model PN, and we see that the observational diagram is well reproduced, while more than 50% of the model PN are density bounded.

Fig. 5 shows the effect of observational selection on the derivation of the PN mass distribution. The thin continuus line represents the original distribution of total nebular masses - i.e. Gaussian in the log, with the parameters given above-. The thick dot-dashed line corresponds to the total nebular masses for those PN with F(6cm) < 10 mJy, while the thick dotted line represents the ionized masses for the same subsample. All three distributions are normalized to 81 objects. The dot-dashed curve is shifted rightwards with respect to the original nebular mass distribution, because the less massive nebulae are generally too faint to be observed. The mean nebular mass corresponding to the observable sample is 0.19 $M_\odot$ while it was 0.13 $M_\odot$ in the original distribution. The distribution of the ionized masses, which are the masses that can be observed, has a long tail towards small masses, constituted of the compact, ionization bounded nebulae.

https://doi.org/10.1017/S0074180900172067 Published online by Cambridge University Press

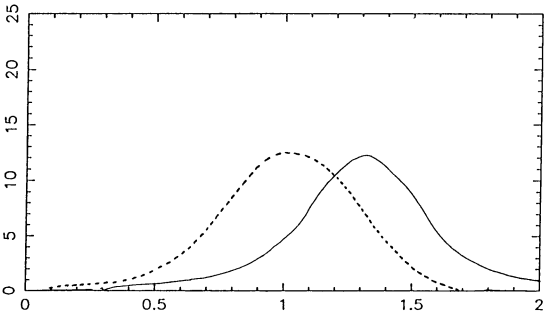

Fig. 6 log v_{exp}

Fig. 6 shows the simulated distribution of log v_{exp}, normalized to 81 PN; thin curve: original population, thick dashed curve: PN with $\phi < 20"$ and F(6cm) > 10mJy. Because PN with large v_{exp} quickly reach a diameter of 20", the latter distribution contains a smaller proportion of rapidly expanding PN than the original distribution. The peak in the distribution lies at ~ 11km/s, instead of 20km/s.

4. DISCUSSION

This very schematic model population is only to be taken as an instructive example. It reproduces quite well the classical observational diagrams shown above, including the M_ϕ vs ϕ relation. This example shows that, because of selection effects, the apparent properties of a sample of PN may be quite different from the characteristics of the underlying PN population.

Real nebulae are neither spherical, nor ionized by blackbodies, and the Schönberner tracks may not be appropriate for at least some PN nuclei (because of the rôle of helium flashes, different mass loss, binary stars). This introduces a scatter which was not taken into account in the simulations. The true nebular mass and expansion velocity distributions should therefore be narrower than assumed in any simulation.

In thesimulated population presented above, 68% of the PN have nebular masses within $\pm$0.3dex of 0.1$M_\odot$. If the true population corresponds to this solution, this would put a strong constraint on dynamical models of the formation of nebular envelopes. The distribution of the PN nuclei masses is also very narrow, with a mean of 0.57 $M_\odot$ in the original distribution (0.58 $M_\odot$ after including selection effects), quite below the value admitted up to now.

However, we stress that the simulated population discussed here may not represent the real one, and we are pursuing this work to explore all the possible solutions. In order to obtain a more reliable picture of the GBPN population, is crucial to extend the sample of GBPN radio observations down to 6 cm fluxes of 1mJy. Indeed, the aspect of the histogram of F(6cm) between 1 and 10mJy is very sensitive to the number of PN ionized by stars of masses higher than 0.61$M_\odot$ as can be seen in diagrams presented by Stasińska et al. (1991). Also, accurate angular diameters are needed for the whole sample. Finally, measurements of the expansion velocities for GBPN, which are presently known for only a few objects, would be most helpful. Indeed, they provide an important constraint, since the expansion velocity determines the epoch when a given PN becomes optically thin.

A complete version of this work will be submitted to Astronomy and Astrophysics.

References

Blöcker T., Schönberner D. (1990) A&A 240, L11
Schönberner D. (1979) A&A 79, 108, (1983) APJ 272, 708
Stasińska G., Tylenda, R., Acker A., Stenholm B. (1989) A&A 247, 173
Stasińska G., Fresneau A., Gameiro, G.F., Acker A. (1991) A&A 252, 762
Zijlstra A.A., Pottasch S.R., Bignell C. (1989) A&A S 79, 329